Research Signpost
37/661 (2), Fort P.O., Trivandrum-695 023, Kerala, India

Surface Tension-Driven Flows and Applications, 2006: 103-120 ISBN: 81-308-0065-9
Editor: R. Savino

4

Thermal convective instabilities in cylindrical enclosures and floating liquid columns under normal and microgravity conditions

M. Lappa
MARS (Microgravity Advanced Research and Support Center)
Via Gianturco 31 - 80146, Napoli, Italy

Abstract

The analysis deals with a comparative study of available theoretical and numerical results about the dynamics of natural (gravitational), Marangoni and related mixed convection in various axisymmetrical geometrical configurations. Emphasis is given to fundamental knowledge provided over the last years by landmark analyses as well as to very recent novel contributions. Attention is focused on the cases of

Correspondence/Reprint request: Dr. M. Lappa, Via Salvator Rosa 53, San Giorgio a Cremano, 80046 – Napoli Italy. E-mail: marlappa@marscenter.it, marlappa@unina.it

cylindrical enclosures and floating zones under different possible heating conditions (lateral heating and heating from below). The differences between gravitational and Marangoni convection are stressed and cross-comparison is used as an useful means to shed additional light on the fundamental nature and structure of both these types of convection in these axisymmetric geometrical models. Silicon melt is considered as a reference case owing to the widespread use of this liquid in various technological processes pertaining to the growth of single-crystalline specimens from initial polycrystalline samples.

1. Introduction

Most technological processes for semiconductor crystal growth from the melt are carried out in axisymmetric configurations (see, e.g., Figs. 1). They require the application of axial and/or radial thermal gradients across the phase boundary; these gradients provide driving forces for free convection in all fluid phases involved. The melt is therefore subject to varying heat- and mass-transfer conditions, which in recent years have been found to be directly or indirectly responsible for a vast majority of bulk deficiencies in single crystalline electronic materials. In particular, instabilities of the melt flow usually lead to three-dimensional (azimuthal) effects which strongly affect the quality of the growing crystals, and therefore are highly undesirable. It is necessary, therefore, to predict the appearance of these instabilities and to understand the related physical mechanisms. Further improvements in this field require, in fact, an exhaustive knowledge of the nature and of the structure of these flows.

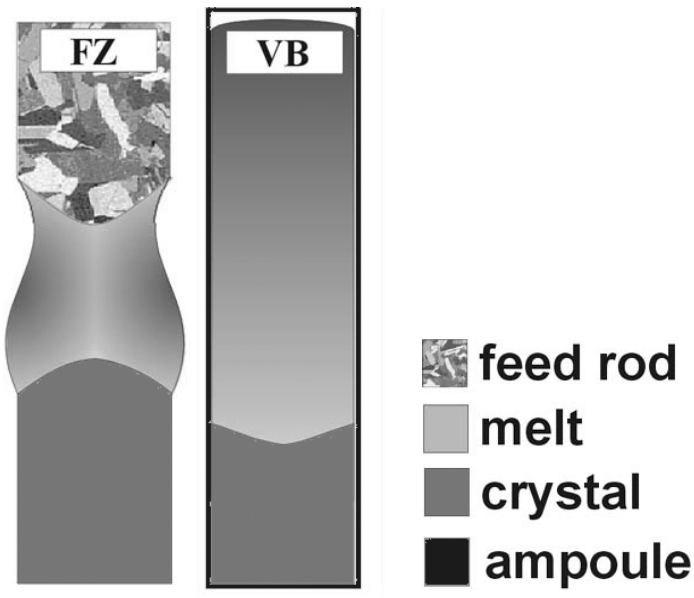

Figure 1. Sketch of the Floating-Zone (FZ) and the Vertical Bridgman (VB) methods.

The FZ technique

During the Floating-Zone (FZ) process a melt zone is established between the lower seed material and upper feed material by applying localized heating (see, e.g. Fig. 1a). This floating zone is moved along the rod (by means of relative motion of the heating device) in such a way that the crystal grows on the seed (which is below the melt) and simultaneously melting the feed material above the floating zone. The seed material as well as the feed rod is supported but no container is in contact with the growing crystal or the melt, which is held in place only by surface tension.

Therefore, the key characteristic of this method of float zoning is that the molten zone does not need to be in contact with a foreign solid (crucible) that, besides being awkward to realize in the practice (the working temperature of the crucible must be well above the 1690 K of the melting temperature of silicon, e.g.), would introduce impurities unacceptable for the applications envisaged (molten silicon is a very reactive material).

Of course, containerless processing on massive samples can only be done in the microgravity environment of space where the forces used for suspending and manipulating the specimens are not overwhelmed by gravity. Microgravity requires much smaller forces to control the position of containerless samples; this also means that the materials being studied are not disturbed as much as they would be if they were levitated on Earth.

Under Earth conditions the zone height is limited because the liquid tends to run down when the molten zone gets too big. This fact limits the possible diameter of crystals. In space the maximum zone height is given by the circumference of the sample; therefore, floating-zone experiments with higher zone heights and larger diameters are feasible under microgravity.

Superimposed on this, is the fact that in such environment, buoyancy forces, that are the most important cause of crystal imperfections on Earth, are absent.

Despite these advantages, however, owing to the presence of a free melt-gas interface, thermal Marangoni convection is induced. Prior to the space program, this phenomenon had been ignored since on the ground it is often overshadowed by the convective flow of gravitational origin. In microgravity, the reduced level of buoyancy-driven convection allowed Marangoni convection to become obvious. Once it became recognized it was found to be significant in many Earth-based processes as well.

Bridgman method (directional solidification)

In Bridgman growth, directional solidification occurs within a vertical ampoule (VB) or a horizontal open boat (HB). The ampoule or boat is inside a furnace with a temperature that varies from above the melting point at one end to below the melting point at the other end. Freezing is

caused by moving the ampoule through a fixed furnace or vice versa, or by slowly lowering the furnace temperature with both ampoule and furnace immobile. This latter method is often called the "gradient-freeze technique" or "power-down method".

In VB (Fig. 1b), the ampoule, which is, for example, a quartz glass or a graphite container, is necessary to support the melt, because, in contrast to the FZ method, the whole feed material (above the crystal) is molten.

The advantages of FZ over Bridgman include the absence of a container in contact with the melt (which normally is the source of impurities in the liquid) and the absence of a container in contact with the processed crystal, which frequently causes stress-induced defects in the crystal because of the different thermal contraction of the crystal and ampoule as they cool.

Under normal gravity conditions, strong fluid motion arises in the melt owing to thermal gravitational convection.

2. Thermal gravitational convection

The relevant nondimensional numbers are the well known Prandtl and Rayleigh numbers

$$\mathrm{Pr} = \frac{\nu}{\alpha} \tag{1}$$

$$Ra = \frac{g\beta_T \Delta T L^3}{\nu\alpha} \tag{2}$$

where ν is the kinematic viscosity, α the thermal diffusivity, β_T the thermal expansion coefficient, ΔT a reference temperature gradient and L a reference length for the geometrical configuration of interest; the Rayleigh number (Ra) can be regarded as a measure of the magnitude of the buoyancy velocity V_g to the thermal diffusive velocity (α/L), where V_g reads

$$V_g = \frac{g\beta_T \Delta T (L)^2}{\nu} \tag{3}$$

Moreover

$$Gr = Ra/\mathrm{Pr} = \frac{g\beta_T \Delta T L^3}{\nu^2} \tag{4}$$

is the Grashof number which represents the ratio of buoyant to molecular thermal transport (only two of the Gr, Ra and Pr numbers are independent).

Onset of gravity-induced convection for different heating conditions (from the side or from below) and for various geometrical configurations is a basic problem in many heat-transfer systems in technical applications and has been widely investigated in the literature. For instance, the behavior of fluids uniformly heated from below falls into the category of phenomena known under the heading of "Rayleigh-Bènard" problem that is one of the most intensively studied hydrodynamical systems. Also, the case of configurations "heated from the side" has instigated much research.

3. Rayleigh-Bènard convection in cylindrical enclosures

It is known (see Touihri et al. [1] and references therein) that the structure of the emerging buoyancy flow, which is given by the first primary threshold, depends on the aspect ratio A (height/diameter). For the case of adiabatic sidewalls, in particular, the flow is axisymmetric for $A<0.55$ ($m=0$) and asymmetric for larger values of A ($m=1$, where m is the number of disturbance nodes in azimuthal direction, also known as "wave number"). Transition between axisymmetric and asymmetric modes occurs around $A=0.72$ if conductive lateral boundaries instead of adiabatic walls are considered.

The thresholds for this primary (steady) instability are independent of the Prandtl number (the critical Rayleigh number behaves merely as an increasing function of the aspect ratio, see Table 1).

Table 1. Critical Rayleigh number versus the geometrical aspect ratio, adiabatic lateral wall, after [1].

A	m	Ra_c
0.5	0	2250
1.0	1	3700

If the Rayleigh number is further increased the flow can undergo a subsequent transition to even more complicated flow patterns. This aspect is still a subject of investigation.

Wanschura et al. [2] made a complete analysis of this secondary instability, but the study was limited to a range of aspect ratio for which the first primary threshold corresponds to steady axisymmetric flow. For this case the unstable mode for the secondary transition is generally a steady mode $m=2$, but it can also be a steady mode $m=1,3$ or 4 according to the

values of the aspect ratio and of the Prandtl number (m=1 and 3 for Pr=0.02 whereas m=4 appears for Pr=1). It was shown that the secondary threshold increases with the Prandtl number and depends also strongly on A. They also elucidated how for large Prandtl numbers, the axisymmetric flow becomes unstable due to the classical thermal (Rayleigh-Bènard) instability mechanism whereas for small Prandtl numbers (liquid metals) the secondary instability is inertial (hydrodynamic) in nature.

Wanschura et al., [2] also investigated the case of liquid bridge (free lateral boundary, i.e. cylindrical or quasi-cylindrical liquid/air interface) showing that, unlike the case with solid boundaries, the onset of pure buoyancy convection in such a configuration is always three-dimensional for any value of the aspect ratio.

4. Buoyancy-convection induced by lateral heating in cylindrical enclosures

Deviation from axisymmetric wall temperature conditions in vertical cylinders was investigated by Pulicani et al. [3] as a possible source of the nonaxisymmetric convection that is often observed during vertical directional solidification experiments.

However, it is worthwhile to stress that even under axisymmetric external conditions, the axisymmetric melt flows can become unstable and bifurcate to asymmetric steady or oscillatory states. This instability of melt flow leads to the appearance of temperature oscillations and asymmetric flow patterns that, in turn, are responsible for the presence of inhomogeneities in the structure of the growing crystals.

Some interesting results concerning the stability of buoyant axisymmetric convection in a vertical cylinder with a parabolic temperature profile at the sidewall have been recently presented by Gelfgat et al. [4] for $0 \leq Pr \leq 0.05$ and $0.5 \leq A \leq 2$. This configuration was studied as a relevant model of the VB technique. The critical parameters corresponding to a transition from the steady axisymmetric (basic state) to the three-dimensional asymmetric (steady or oscillatory) flow pattern were computed and it was elucidated that the instability of the flow is three-dimensional for the whole range of governing parameters studied. In particular, the axisymmetric flow in relatively shallow cylinders tends to be oscillatory unstable via an hydrodynamic Hopf bifurcation of the circulating flow, while in tall cylinders the instability sets in due to a steady bifurcation caused by the Rayleigh-Bènard mechanism. In the first case the three-dimensional perturbation has the form of a traveling wave; accordingly the oscillatory perturbation patterns (as well as the oscillatory component of the flow) rotate around the axis with the angular velocity $2\pi f/m$ (where f is the frequency of the oscillations).

This analysis also predicted the possible existence of very complex three-dimensional behaviors for fixed values of the aspect ratio with the possibility of an adjustment in the number of azimuthal disturbance nodes as the value of the Rayleigh number is varied in a restricted range: For instance, for A=0.5 the critical Rayleigh numbers, that correspond to the azimuthal modes with m=2 and m in the range 5-10 (m is the number of disturbance nodes in azimuthal direction like the case of cylinders heated from below), are relatively close and grow rapidly with the increase of Pr. For this reason for Pr<0.02 a complex interaction of several azimuthal modes at relatively large supercriticalities is possible. As an example, the most dangerous modes for Pr=0.01 are shown in Table 2.

Table 2. Excitation of the most dangerous modes for the laterally-heated cylindrical enclosure (A=0.5, Pr=0.01, Gelfgat et al. [4]).

Ra	m
$Ra \cong 3\cdot 10^3$	4
$Ra \cong 3.7\cdot 10^3$	2
$4.5\cdot 10^3 < Ra < 5\cdot 10^3$	5-10

5. Marangoni convection and possible models of the FZ technique

In addition to the Prandtl number (eq. (1)), the following nondimensional numbers are of particular importance (σ_T is the surface tension derivative):

$$\mathrm{Re} = \frac{\sigma_T \Delta T L}{\rho \nu^2} \tag{5}$$

$$Ma = \mathrm{Re}\cdot \mathrm{Pr} = \frac{\sigma_T \Delta T L}{\mu \alpha} \tag{6}$$

The Reynolds number (Re) measures the magnitude of the tangential stress $\sigma_T \Delta T/L$ to the viscous stress $\rho\nu^2/L^2$; the Prandtl number (Pr) measures the rate of momentum diffusion ν to that of heat diffusion α, and the Marangoni number is Ma=Re·Pr. Only two of these three numbers are independent.

The appropriate scaling of the dimensional velocity is the Marangoni velocity:

$$V_{Ma}^T = \frac{\sigma_T \Delta T}{\mu} \tag{7}$$

Therefore, the Marangoni number can also be regarded as the measure of the relative importance of the Marangoni and of the thermal diffusion velocities.

Two fundamental models of the FZ technique have been introduced over the last years for capturing the underlying relevant fluid-dynamics in terms of basic flow, related transitions and bifurcations (see Figs. 2).

The half-zone model (Fig. 2a) simulates half of a real floating zone (the liquid between one of the ends of the domain and the equatorial plane); it consists of a pair of coaxial, differentially heated cylindrical disks with a bridge of liquid material suspended between them (heat flow is usually neglected through the free surface).

The ends of the full-zone are plane and isothermal as in the case of the half-zone, but the supporting disks are posed at the same temperature (Fig.2b). The presence of a ring heater around the equatorial plane of the zone is simulated by imposing a specified heat flux distribution on the free surface with a maximum of the flux in correspondence of the equatorial plane.

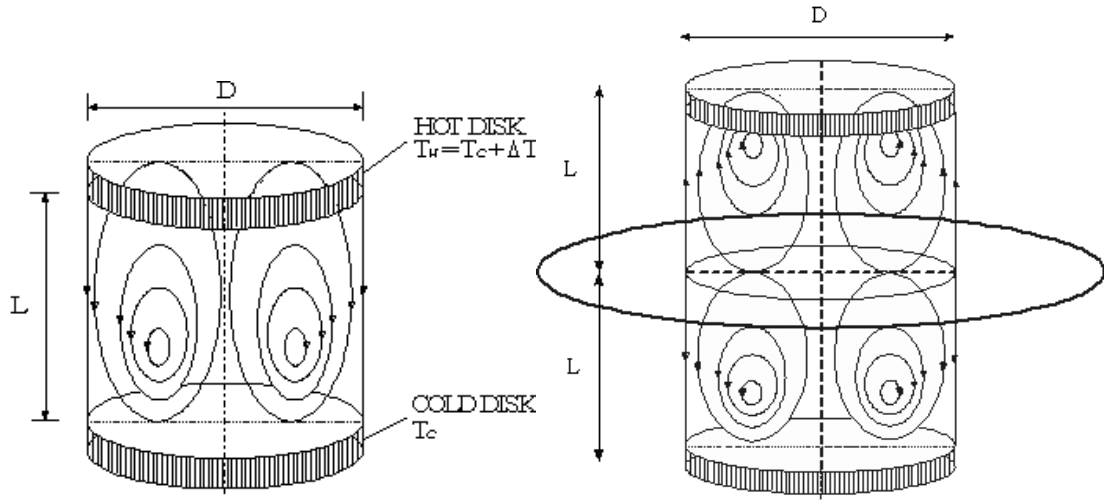

Figure 2. a) The half-zone and its typical boundary conditions b) The full-zone heated by an equatorial ring heater.

Some typical geometrical parameters pertaining to these systems are given below: the geometrical aspect ratio of the liquid column of full-zone extent (A_F) is defined as A_F =2L/D; the aspect ratio of the corresponding half-zone is defined as A_H =L/D= A_F/2 (D is the diameter of the supporting disks); the so-called volume or shape factor S is given by the ratio of the effective volume of liquid held between the supporting disks and the volume of the corresponding straight configuration with cylindrical liquid/air interface (unlike the cylindrical enclosure treated in sections 3 and 4, there is no constraint forcing the lateral boundary to be straight in the FZ case: convex and concave shapes are also possible).

6. Half-zone-based results

Experiments [5-7] performed with transparent organic fluids (characterized by Prandtl numbers higher than those typical of liquid metals) showed that for sufficiently small values of the Marangoni number, the convection in liquid columns (half-zone configuration) heated from above or from below, is laminar, steady and axisymmetrical, but when the Marangoni number exceeds certain critical values (the so-called critical Marangoni number Ma_c) depending on Pr, A_H, S and the imposed ΔT, the liquid motion can undergo a transition to an oscillatory three-dimensional (3D) complex flow pattern.

The appearance of these instabilities in organic liquids was initially used by the investigators (in the 80's) to provide a possible explanation for the undesired microscopic imperfections found in the final crystals obtained in microgravity conditions and even under normal gravity conditions in situations where the Marangoni flow is emphasized with respect to buoyancy forces (microscale experimentation).

Additional research carried out in the subsequent years pointed out, however, that the choice of the proper model liquid is a very delicate aspect of the problem. As highlighted by many linear stability analyses (see, e.g., Kuhlmann and Rath [8]), in fact, the instability of Marangoni flows is initiated through different mechanisms according to the liquid used; by means of an energy analysis, in particular, Wanschura et al. [9] elucidated that the first bifurcation of the flow is due to inertia instability of the axial shear layer below the free surface for small Pr fluids (semiconductor melts and liquid metals) and hydrothermal wave for large Pr fluid (transparent organic liquids) case.

The instability is hydrothermal in nature for $Pr>>1$ (for this case it is strictly related to the coupling and interplay between the velocity and temperature fields) and hydrodynamic in nature for $Pr<<1$ (i.e. it does not depend on the behavior of the temperature field that in this case simply acts as a driving force for the velocity field).

These theoretical analyses also elucidated that for transparent organic liquids the transition to 3D flow is always associated with the onset of oscillatory flow (Hopf bifurcation) whereas for semiconductor melts the instability breaks the spatial axisymmetry (but the flow regime is still steady, stationary bifurcation) prior to the onset of time dependent flow field.

For the first case, in particular, Kuhlmann and Rath [8] found that the 3D supercritical state after the Hopf bifurcation point, is given by superposition of two counter-propagating hydrothermal waves, with axial and azimuthal components similar to those already disclosed in the landmark investigation of Smith and Davis [10] in the case of infinite horizontal liquid layers.

In principle, if the two waves have equal amplitudes the resulting disturbance is a "standing wave", with the minimum and maximum disturbances pulsating at fixed azimuthal positions; while the superposition of waves with different amplitude gives rise to a "traveling wave", with the minimum and maximum disturbances traveling in the azimuthal direction.

However, owing to an intrinsic limitation of the method employed (that is based on simplified equations), linear stability analyses cannot provide additional information about the effective occurrence of these regimes (since no prediction is possible about the amplitude of the disturbances).

The experiments performed on the ground and in microgravity conditions revealed one or the other mode of convection. The results concerning $Pr>>1$ are no longer discussed herein since they are not applicable to semiconductor melts.

For liquid metals, outstanding pioneering numerical studies for microgravity conditions were carried out by Rupp et al. [11] and Levenstan and Amberg [12]. The free interface was assumed to be cylindrical in these studies and the azimuthal wave number (m) was found to behave as a decreasing function of the aspect ratio, i.e. $2mA=const$ (see also Table 3); Lappa and Savino [13] extended such a relationship to the case of dynamical aspect ratio changes induced by solidification.

Imaishi et al. [14] depicted in detail the complex spatio-temporal evolution of the flow field that occurs after the secondary (oscillatory, $Ma>Ma_{c2}$) bifurcation of the Marangoni flow for different values of the aspect ratio A and of the Prandtl number ($0\leq Pr\leq 0.02$), elucidating different (referred to as "torsional") oscillatory behaviors.

The effect of a noncylindrical shape was considered by Lappa et al. [15] and Chen et al. [16] for the first bifurcation. They found (half-zone under microgravity) that for a fixed aspect ratio the critical azimuthal wave number can be shifted to higher values by increasing S (convex shape) or to lower values by decreasing S (concave shape).

Table 3. Critical Marangoni number versus the geometrical aspect ratio, Pr=0.01, S=1, microgravity conditions (results of Imaishi et al. [14]; Chen et al. [16]).

A_H	m	Ma_{c1}
0.4	2	27.0
0.5	2	20.8
0.6	2	15.8
0.7	2	12.6
0.8	2	12.0
0.9	1	10.1

7. The half-zone heated from below

With regard to effect of gravity, some interesting results about liquid bridges (A_H=1, L= 1 [cm]) heated from above or from below in the case of low-Pr fluids were yielded by Lappa et al. [17].

According to their simulations if the deformation of the shape induced by gravity is taken into account (amphora-like), gravity always acts stabilizing the Marangoni flow regardless of the direction of the gravity vector (parallel or antiparallel to the axis), whereas in the unrealistic case of a straight surface the heating from below condition leads to destabilization of the flow. The on-the-ground deformation of the shape also influences the azimuthal organization of the flow field. The azimuthal wave number is shifted to higher values if the heating from above condition is considered (see the last two columns in Table 4).

Among other things, this study also disclosed that the steady (first) bifurcation in liquid bridges heated from below with pronounced shape deformation (e.g., Gallium half-zone with height 1 [cm]) is suppressed; in this case, in fact, the flow undergoes a direct transition to oscillatory flow with hydrodynamic pulsating and rotating modes of convection. These regimes are qualitatively similar to those usually observed in the case of high Prandtl number liquids and hydrothermal behaviors (see Figs. 3 and 4).

Table 4. Critical Marangoni number for the half-zone under normal gravity conditions (L= 1 [cm], A_H=1, S=1, Silicon, Pr=0.01) after Lappa et al. [17].

	Cylinder 1g Heating from above	Cylinder Zero g	Cylinder 1g Heating from below	1g shape Heating from above	1g shape Heating from below
Ma_{c1}	15.36	15.24	14.92	16.62	18.78
m	1	1	1	2	1

Figure 3

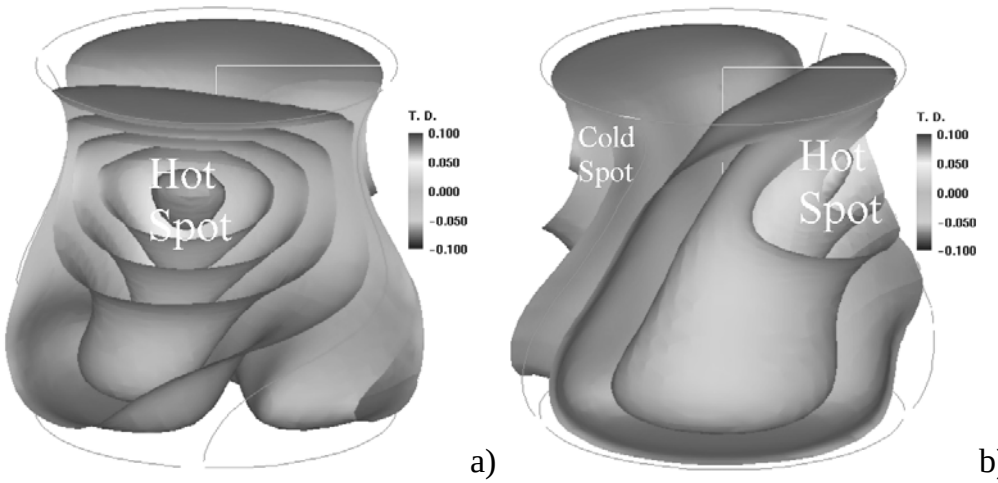

a) b)

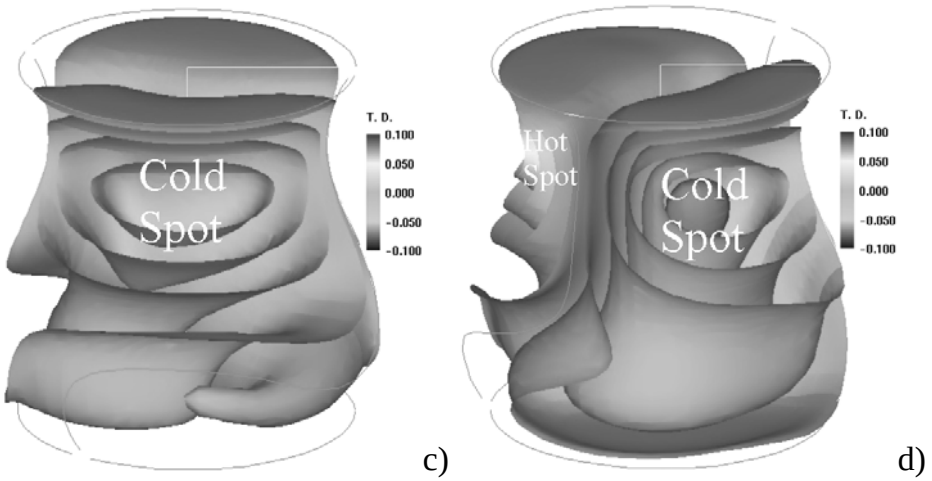

Figure 3. Snapshots of temperature-disturbance isosurfaces over a period of oscillation (Ma=300, gallium liquid bridge, 1g, heating from below, rotating regime).

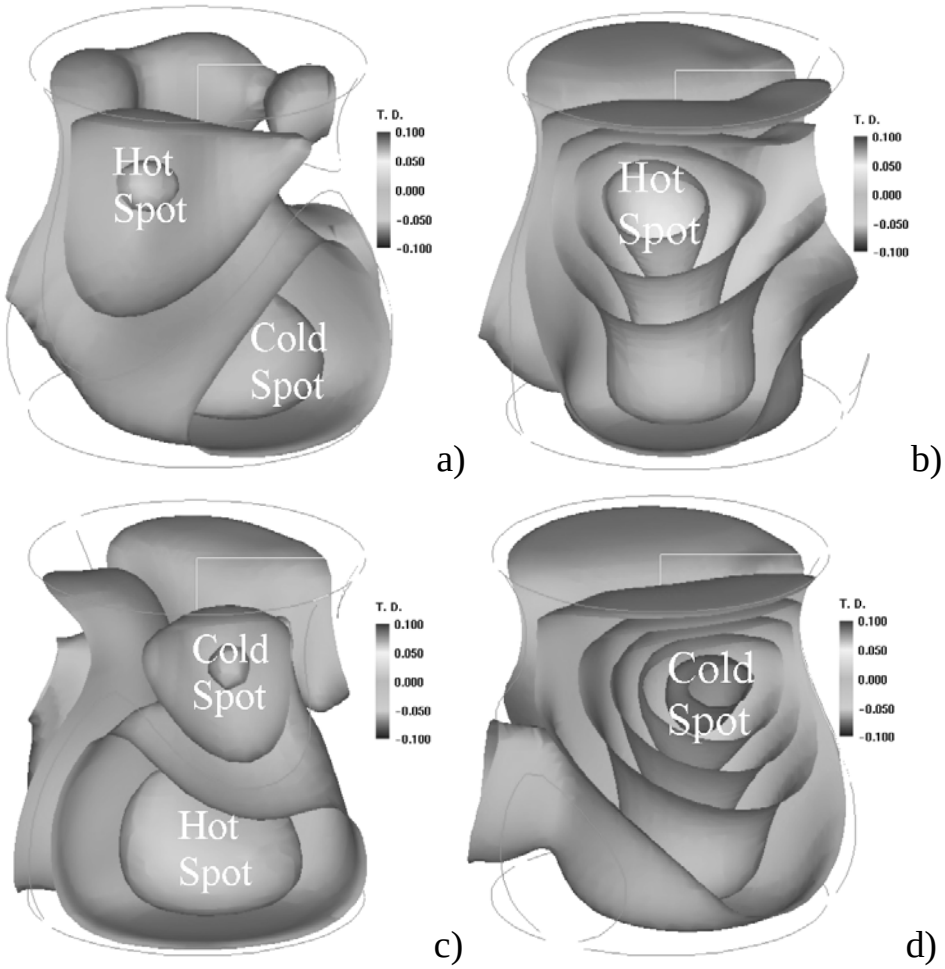

Figure 4. Snapshots of temperature-disturbance isosurfaces over a period of oscillation (gallium liquid bridge, 1g, Ma=300, heating from below, pulsating regime).

8. The full-zone with lateral heating

Cylindrical interface and microgravity conditions

The major outcome of computations carried out for the full-zone under the constraint of cylindrical interface and zero-g conditions is that for both even and odd critical azimuthal wave numbers the mirror symmetry with respect to the mid-plane is broken (see, e.g., Fig. 5 showing the surface azimuthal velocity).

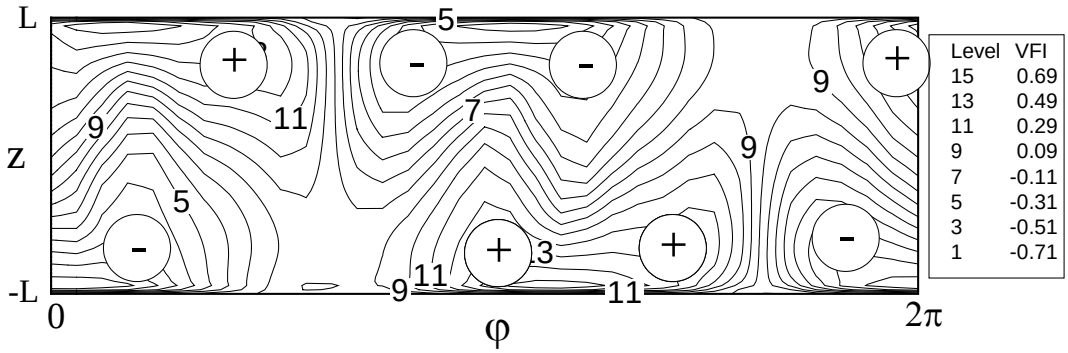

Figure 5. Surface azimuthal velocity distribution at the 3D stationary state (A_F=1.3, m=1, Ma≅30, zero-g).

This finding is of paramount importance if one considers that, in the light of this result, the half-zone (supposed to model the flow in a half of the real floating zone under the constraint that this flow is symmetric by reflection about the plane at mid-height between the rods) should not be used to obtain quantitative data about the FZ technique.

The aforementioned symmetry breaking is the main reason why the Ma_{c1} values computed for the cylindrical half-zone model by several investigators (e.g., Table 3) are two times higher than the values recently calculated for the case of full-zone model (Table 5). The flow symmetry with respect to the mid-plane is an additional and relevant part of the problem. It indeed introduces a new degree of freedom. The differences between the two configurations, however, are not limited to this feature (see the next section).

Concave and convex volumes in microgravity

As mentioned in section 6 in the case of liquid metals and half-zone, for a fixed aspect ratio the critical azimuthal wave number can be shifted to higher values by increasing S (convex shape) or to lower values by decreasing S (concave shape). The full-zone exhibits quite a different behavior since the azimuthal wave number increases in case of deviation from a volume equal to the cylindrical one for both cases S<1 and S>1 (Tables 6 and 7).

Table 5. Critical azimuthal wave number and critical Marangoni number versus the aspect ratio (Pr=0.01, full-zone, S=1, microgravity conditions, Lappa [18]).

$A_F=2A_H$	L [cm]	m	Ma_{c1}
0.2	0.1	9	22.157
0.3	0.15	6	15.340
0.4	0.2	4	12.280
0.5	0.25	4	9.760
0.6	0.3	3	13.597
0.7	0.35	2	10.90
0.8	0.4	2	12.028
0.9	0.45	2	11.326
1.0	0.5	2	12.413
1.1	0.55	2	14.910
1.2	0.6	2	15.086
1.3	0.65	1	11.350
1.5	0.75	1	10.154
1.8	0.9	1	10.364
2.0	1.0	1	9.923

Table 6. Critical azimuthal wave number and critical Marangoni number versus the volume of the liquid zone (Pr=0.01, full-zone, microgravity conditions, Lappa [19]).

A_F	L [cm]	$S=V/V_o$	m	Ma_{c1}
1.0	0.5	0.80	4	48.08
1.0	0.5	0.85	3	34.59
1.0	0.5	1	2	12.41
1.0	0.5	1.2	2	6.85
1.0	0.5	1.3	2	10.87
1.5	0.75	1	1	10.15
1.5	0.75	1.2	1	1.45
1.5	0.75	1.4	2	11.53

Table 7. Critical azimuthal wave number and critical Marangoni number versus the volume of the liquid zone (Pr=0.01, full-zone, L=0.5 [cm], A_F =1.0, on the ground conditions, after Lappa [20]).

S=V/Vo	m	Ma_{c1}
0.80	3	33.24
0.85	3	27.99
0.90	2	12.39
1	1	8.40
1.1	1	3.31
1.2	2	9.54

The new degree of freedom plays a crucial role also with regard to these aspects: In principle each convection roll is bounded by a wall from one side and it is free to interact in non linear way with the opposite convection roll from the other side. It can puff up crossing the mid-plane and protruding in the opposite side of the liquid zone; however this degree of freedom is somewhat reduced in the case S<1. In such case, in fact, due to the concave shape of the free surface, the convection rolls are confined each to the respective half of the full-zone configuration (Fig. 6a; this prevents mutual interference and strengthens the constraints for the flow field leading to a larger value of the critical Marangoni number). On the contrary, for S>1 each toroidal roll is free to interact with the opposite roll and to become pervasive throughout the system (Fig. 6c) lowering the stability threshold.

Such an interaction is also responsible for the "apparent" doubling of the azimuthal wave number in the mid-plane shown in Fig. 6d (see Lappa [18] for additional details).

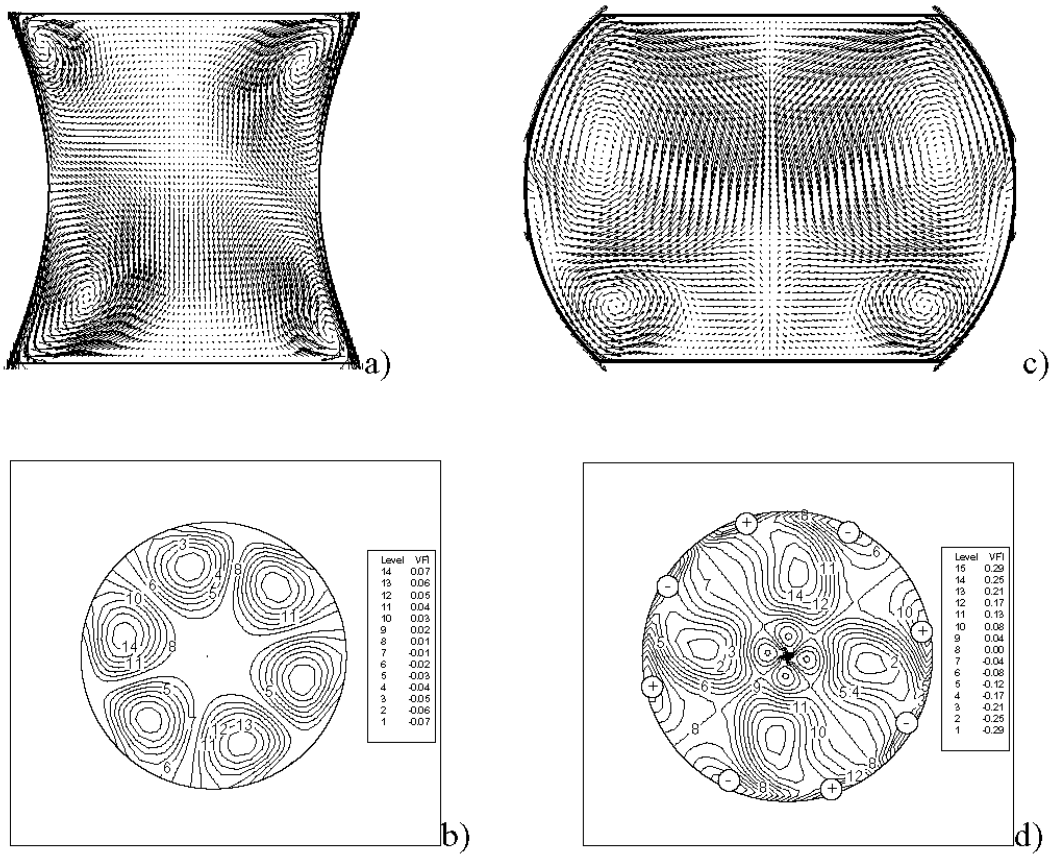

Figure 6. On the left, structure of 3D Marangoni flow with m=3, A_F =1.0, S=0.85, Ma=50, zero-g: (a) velocity field in the generic meridian plane; (b) azimuthal velocity in the equatorial plane. On the right, structure of 3D Marangoni flow with m=2, A_F=1.0, S=1.3, Ma=25, zero-g; (c) velocity field in the generic meridian plane; (d) azimuthal velocity in the equatorial plane (the wave number therein seems to be m=4).

On the ground conditions

Comparison between Tables 6 and 7 gives insights into the effect of gravity on the features of the instability of Marangoni flow in liquid floating columns of full extent.

For a volume equal to the cylindrical one the on the ground Marangoni flow is destabilized with respect to microgravity conditions and the azimuthal wave number is shifted to a lower value. The same trend occurs in the case of $S<1$; gravity acts destabilizing the Marangoni flow and shifting the azimuthal wave number to lower values. Vice versa stabilization occurs in the case $S>1$.

For the half-zone, the trend is completely different as previously discussed in section 7.

It is worthwhile to stress that, however, if the analysis is limited to the primary bifurcation, for both cases of half- and full-zones, the key factor at the root of the behaviors illustrated above is the influence exerted on the system by the amphora-like configuration of the free surface, whereas the role played by the buoyancy effect per se can be regarded as almost negligible (Lappa [21]).

At this stage it is necessary to open a short discussion about the strategies by which these delicate effects can be properly evaluated.

In the case of high Prandtl number liquid bridges the method basically relies on the cross-comparison of experimental results obtained in the opposite situations of heating from above and heating from below (e.g., Velten et al. [6]).

A simple procedure for the critical estimation of the buoyancy effects in zones of full extent can be based on neglecting the Boussinesq term in the Navier-Stokes equations. Numerical simulations repeated after "switching off" this term show, in fact, that for low values of the imposed temperature difference (i.e. near the threshold of the first bifurcation), the buoyancy forces weakly affect the flow field (the difference between the results lies below 3%). This means, as anticipated, that for very low values of the Marangoni number (i.e. of the temperature gradient acting along the melt/gas interface), the main effect of the gravitational field on the features of the instability for low-Pr fluids is exerted through its influence on the shape of the free surface.

9. Conclusions

The understanding of the relevant mechanisms at the root of flow instabilities in relevant geometrical models of crystal growth processes from the melt, is of paramount importance. It can be regarded as the necessary basis of any attempt devoted to the precise definition of

operating parameters that may provide a stable melt flow pattern under the required technological conditions and/or to the introduction of possible strategies for control of melt convection. In the present review a quite exhaustive picture of the different fluid-dynamic mechanisms (and related "ranges" of applicability) responsible for onset of flow and related bifurcations in axisymmetric configurations has been provided together with precise quantitative data about the first threshold of instability.

An obvious justification for the long lasting (and continuing) efforts in these fields can be found, as mentioned above, in the relevance that these phenomena have in several industrial applications. However, it is rather clear that these problems have also exerted an appeal on scientists and engineers as a consequence of the complexity of the possible stages of evolution and of the non-linear behavior. This complexity is shared with other systems in nature and still constitutes a remarkable challenge for any theoretical model [22].

10. References

1. Touihri R., Ben Hadid H., Henry D., (1999), "On the onset of convective instabilities in cylindrical cavities heated from below. I. Pure thermal case", Phys. Fluids, 11 (8): 2078-2088.
2. Wanschura M, Kuhlmann H. C., Rath H. J., (1996), "Three-dimensional instability of axisymmetric buoyant convection in cylinders heated from below", J. Fluid Mech., 326: 399:415.
3. Pulicani J.P., Krukowski S., Alexander J. I.D., Quazzani J., Rosenberger F., (1992), "Convection in an asymmetrically heated cylinder", Int. J. Heat Mass Transfer, 35(9): 2119-2130.
4. Gelfgat A.Yu., Bar-Yoseph P.Z., Solan A., (2000), "Axisymmetry breaking instabilities of Natural convection in a vertical Bridgman growth configuration", J. Cryst. Growth 220: 316-325.
5. Preisser F., Schwabe D., Scharmann A., (1983), "Steady and oscillatory thermocapillary convection il liquid columns with free cylindrical surface", J. Fluid Mech., 126: 545-567.
6. Velten R., Schwabe D., Scharmann A., (1991), "The periodic instability of thermocapillary convection in cylindrical liquid bridges", Phys. Fluids A 3: 267-279.
7. Frank S., Schwabe D., (1998), "Temporal and spatial elements of thermocapillary convection in floating zones", Experiments in Fluids, 23: 234-251.
8. Kuhlmann H.C., Rath H.J., (1993), "Hydrodynamic instabilities in cylindrical thermocapillary liquid bridges", J. Fluid Mech., 247: 247-274.
9. Wanschura M., Shevtsova V., Kuhlmann H.C., Rath H.J., (1995), "Convective instability mechanism in thermocapillary liquid bridges", Phys. Fluids, 5: 912-925.
10. Smith M.K., Davis S.H. (1983), "Instabilities of dynamic thermocapillary liquid layers. Part 1 : convective instabilities ", J. Fluid Mech 132: 119-144.

11. Rupp R., Muller G., Neumann G., (1989), "Three dimensional time dependent modelling of the Marangoni convection in zone melting configurations for GaAs", J. Cryst. Growth, 97: 34-41.
12. Levenstam M., Amberg G., (1995), "Hydrodynamical instabilities of thermocapillary flow in a half-zone", J. Fluid Mech. 297: 357-372.
13. Lappa M., Savino R., (2002), "3D analysis of crystal/melt interface shape and Marangoni flow instability in solidifying liquid bridges", J. Comput. Phys. 180 (2): 751-774.
14. Imaishi N., Yasuhiro S., Akiyama Y. , Yoda S., (2001), "Numerical simulation of oscillatory Marangoni flow in half-zone liquid bridge of low Prandtl number fluid"; J. Crystal Growth, 230:164-171.
15. Lappa M., Savino R. and Monti R., (2001), "Three-dimensional numerical simulation of Marangoni instabilities in non-cylindrical liquid bridges in microgravity"; Int. J. Heat Mass Transfer, 44, (10): 1983-2003.
16. Chen Q.S., Hu W.R., Prasad V., (1999), "Effect of liquid bridge volume on the instability in small-Prandtl-number half zones", J. Cryst. Growth, 203: 261-268.
17. Lappa M., Yasushiro S., Imaishi N., (2003), "3D numerical simulation of on ground Marangoni flow instabilities in liquid bridges of low Prandtl number fluid", Int. J. Num. Meth. Heat Fluid Flow 13 (3): 309-340.
18. Lappa M., (2003), "Three-dimensional numerical simulation of Marangoni flow instabilities in floating zones laterally heated by an equatorial ring", Phys. Fluids 15 (3): 776-789.
19. Lappa M., (2005), "Analysis of flow instabilities in convex and concave floating zones heated by an equatorial ring under microgravity conditions", Computers & Fluids - 34(6): 743-770.
20. Lappa M., (2004), "Combined effect of volume and gravity on the three-dimensional flow instability in non-cylindrical floating zones heated by an equatorial ring", Phys. Fluids 16 (2): 331-343.
21. Lappa M., (2004), "Floating zones heated around the equatorial plane: models and simulations", Microgravity Science & Technology, XV/3: 36-51.
22. Lappa M., (2005), "On the nature and structure of possible three-dimensional steady flows in closed and open parallelepipedic and cubical containers under different heating conditions and driving forces", Fluid Dynamics & Materials Processing, 1(1): 1-19.